

## Original Research

# A combinatorial drug screen in PDX-derived primary rhabdomyosarcoma cells identifies the NOXA - BCL-XL/MCL-1 balance as target for re-sensitization to first-line therapy in recurrent tumors ☆☆☆



Gabriele Manzella<sup>a</sup>; Devmini C. Moonamale<sup>a</sup>; Michaela Römmele<sup>a</sup>; Peter Bode<sup>b</sup>; Marco Wachtel<sup>a</sup>; Beat W. Schäfer<sup>a,\*</sup>

<sup>a</sup> Department of Oncology and Children's Research Center, University Children's Hospital, Zurich, Switzerland

<sup>b</sup> Department of Pathology and Molecular Pathology, University Hospital Zurich, Zurich, Switzerland

## Abstract

First-line therapy for most pediatric sarcoma is based on chemotherapy in combination with radiotherapy and surgery. A significant number of patients experience drug resistance and development of relapsed tumors. Drugs that have the potential to re-sensitize relapsed tumor cells toward chemotherapy treatment are therefore of great clinical interest. Here, we used a drug profiling platform with PDX-derived primary rhabdomyosarcoma cells to screen a large drug library for compounds re-sensitizing relapse tumor cells toward standard chemotherapeutics used in rhabdomyosarcoma therapy. We identified ABT-263 (navitoclax) as most potent compound enhancing general chemosensitivity and used different pharmacologic and genetic approaches *in vitro* and *in vivo* to detect the NOXA-BCL-XL/MCL-1 balance to be involved in modulating drug response. Our data therefore suggests that players of the intrinsic mitochondrial apoptotic cascade are major targets for stimulation of response toward first-line therapies in rhabdomyosarcoma.

*Neoplasia* (2021) 23, 929–938

**Keywords:** Rhabdomyosarcoma, PDX-derived primary cells, BCL-2 family proteins, Re-sensitization, Recurrent tumors

## Introduction

Chemotherapy has dramatically improved the survival rate of patients with different types of tumors. In particular, this includes different pediatric tumors such as some leukemia and sarcoma. However, failure of conventional treatment in high-risk patients remains a major unsolved clinical problem also

in these entities. Responsible for relapse tumor growth is initial or acquired resistance to chemotherapy. At the molecular level, a plethora of different mechanisms have been identified that can lead to chemoresistance [1]. Hence, novel treatment strategies to overcome chemoresistance are urgently needed. One potential approach is the use of drugs that re-sensitize cancer cells toward first-line chemotherapies (re-sensitizers) when applied as combination therapy. Alternatively, first-line therapies might be completely replaced by drugs affecting alternative pathways.

Rhabdomyosarcoma (RMS) is the most common pediatric soft tissue sarcoma. RMS is further subdivided based on histologic characteristics into several subgroups, with embryonal (ERMS) and alveolar RMS (ARMS) being the most frequent ones. While most ARMS harbor the specific fusion proteins PAX3/7-FOXO1 (fusion-positive RMS; FP-RMS), ERMS have frequent mutations in the RAS pathway but are not associated with fusion proteins (fusion-negative RMS; FN-RMS). Despite intense search for more specific therapies during the past 2 decades, current first-line treatment regimens for RMS are still based on a combination of chemotherapy, radiotherapy and surgery. Standard chemotherapy for RMS involves a combination of drugs, with vincristine, actinomycin d, and cyclophosphamide (VAC) as

\* Corresponding author.

E-mail address: [Beat.Schaefer@kispi.uzh.ch](mailto:Beat.Schaefer@kispi.uzh.ch) (B.W. Schäfer).

☆ Funding: The work was supported by grants from the Swiss National Science Foundation (3100-156923 and 3100-175558) and the Childhood Cancer Research Foundation Switzerland to BS.

☆☆ Declaration of Competing Interest: The authors declare that they have no known competing financial interests or personal relationships that could have appeared to influence the work reported in this paper.

Received 16 March 2021; received in revised form 15 June 2021; accepted 2 July 2021

© 2021 The Authors. Published by Elsevier Inc. This is an open access article under the CC BY-NC-ND license (<http://creativecommons.org/licenses/by-nc-nd/4.0/>) <https://doi.org/10.1016/j.neo.2021.07.001>

backbone, a combination that has not changed for more than 40 y [2]. However, 30% of RMS patients relapse and the survival rate of these patients is less than 20% [3,4], a situation that has not changed over the past 2 decades.

Many potential alternative drugs have been tested *in vitro* for RMS treatment during this time, however no real breakthrough was achieved up to now. It is widely accepted that one of the reasons for the high rate of failure has been the lack of preclinical models that accurately recapitulate all characteristics of human tumors. Especially cell line-based models, which have been mainly used in the past, have been questioned. They do not represent the heterogeneity of tumor cohorts found among human patients and furthermore, during the long time since their generation, they underwent a continuous adaption and evolution process *in vitro*, that can lead to a large divergence from the tumors cells they originate from [5,6]. However, the development of personalized model systems in the recent years including patient-derived xenografts (PDX) and short-term *in vitro* cultures of primary, patient-derived cells in 2D or 3D (organoids or spheroids) has set the basis for the discovery of more effective drugs in the future [7,8].

We recently established a drug profiling platform for primary RMS cells [9]. We optimized culture conditions for cells isolated from patient-derived xenografts (PDX) or directly from human patient tumors that allow continuous propagation of the cells while maintaining their molecular characteristics. These cells can be used to evaluate the response toward a large collection of drugs in a high-throughput manner. This platform therefore represents a step toward more personalized therapies for RMS patients.

Here, we used this platform with cultures from diagnostic and relapse samples from the same patients for screening of small molecule re-sensitizers to first-line chemotherapeutics. Among 204 tested drugs, we detected the BCL-2 family inhibitor ABT-263 (navitoclax) as the most potent re-sensitizer of relapse RMS cells toward treatment with vincristine, etoposide and doxorubicin. We further validated this finding using different pharmacologic and genetic approaches and identified a network of NOXA, MCL-1 and BCL-XL as relevant regulator of cell death during combination treatment with chemotherapeutics and ABT-263. Finally, we tested the combination of ABT-263, and vincristine in a PDX model *in vivo*.

Overall, our data suggest that especially BCL-XL and MCL-1 are promising drug targets in combination with first-line chemotherapy in RMS.

## Results

### *Combination screen identifies ABT-263 as re-sensitizer of recurrent PDX-derived primary cells to first-line treatments*

To address the problem of chemoresistance in RMS and generate a relevant *in vitro* model system, we first asked whether PDX-derived primary cells (PPCs) could recapitulate patient responses to chemotherapies. We tested 2 sets of PPCs (Supplemental Fig. 1) with available pre-treatment and post-relapse samples (SJRHB13758\_X and SJRHB012) by generating dose response curves after 72 hours (h) treatment with different chemotherapeutics. In case of SJRHB13758\_X, which originates from a patient who experienced 21-wk treatment with conventional cytotoxics (Fig. 1A), we observed a clear refractory response to the drugs in recurrent cells compared to their diagnostic PPC (increase in  $IC_{50}$ -doxorubicin >33.8-fold and in  $IC_{50}$ -etoposide >39.9-fold;  $P < 0.01$ ), while in case of SJRHB012 there was no clear difference between diagnostic and relapse sample (Fig. 1B-C and Supplemental Fig. 2). PDXs from the relapse biopsy of the former case (SJRHB13758\_X2) grew faster in mice than cells from the diagnostic biopsy (SJRHB13758\_X1) and reached 100% engraftment (6 out of 6) within 28 d compared to 33% engraftment (2 out of 6) after 140 d (Fig. 1D), respectively, highlighting the more aggressive phenotype of the relapse cancer

cells. Together, this indicates that our *in vitro* PPC maintain, and reflect drug sensitivities as observed in patients.

To identify drugs re-sensitizing toward first-line therapy, we used a library of 204 drugs which contains experimental compounds covering a broad range of molecular pathways as well as many FDA-approved drugs and conventional chemotherapeutics. The library in a concentration of 500 nM was combined with low dose of standard cytotoxic agents (100 nM doxorubicin (- $IC_{20}$ ) or 1  $\mu$ M etoposide (- $IC_{30}$ )) in resistant (SJRHB13758\_X2C) cells and cell viability was assessed 72h post-treatment. We identified 3 drugs which reduced cell viability by at least 40% in combination with etoposide and 6 in combination with doxorubicin, compared to single treatment (Fig. 2A; single agents killing more than 90% are not taken into account). Five out of these 9 drugs target signaling pathways, while 2 directly affect cell death pathways (ABT-263 and BV-6). The only candidate shared between the 2 screens was ABT-263, an inhibitor of the anti-apoptotic proteins BCL-2/BCL-XL/BCL-W. To validate this hit, we performed combinatorial treatments with ABT-263 at 250nM and 500nM and 3 chemotherapeutics (doxorubicin, etoposide and vincristine). These combinations were highly effective, especially in case of vincristine (Fig. 2B). Similar effects were observed in a second relapse sample (SJRHB012\_ZC) (Fig. 2C). To assess induction of apoptosis, we monitored Caspase 3/7-activity upon co-treatment of ABT-263 with doxorubicin (3 to 6h), vincristine (9h) and etoposide (24 to 48h) (Fig. 2D, 2E and Supplemental Figure S3). This revealed that both relapse PPCs had elevated caspase activity when co-treated (-2- to -18-fold) compared to chemotherapy alone. These findings were further corroborated by Western blot analysis, which showed increased levels of cleaved Caspase 3/PARP in co-treated compared to single treated cells (Fig. 2F and 2G). Taken together, these data indicate that ABT-263 re-sensitizes recurrent PPCs to conventional chemotherapeutics by augmenting apoptosis.

### *ABT-263 re-sensitizes RMS cells to chemotherapy via the NOXA/BCL-XL axis*

Since ABT-263 antagonizes several pro-survival BCL-2 family members including BCL-2, BCL-XL and BCL-W, we next used selective inhibitors of either BCL-2 (ABT-199, venetoclax) or BCL-XL (A-1331852). Co-treatment with increasing concentrations of doxorubicin and vincristine for 24h revealed that only pharmacologic inhibition of BCL-XL but not BCL-2 could phenocopy the effects of ABT-263 (Fig. 3A-D), demonstrating that BCL-XL is the relevant player in our PPC models.

Since also chemotherapy treatment can affect expression of BCL-2 family members [10], we next attempted to dissect the anti-apoptotic factors affected by standard chemotherapy. To this aim, we measured expression levels of BCL-2 family members after short-term treatment with doxorubicin and vincristine by Western Blot. Interestingly, treatment with doxorubicin induced a striking down-regulation of MCL-1 expression in 2 recurrent PPCs (Fig. 3E) but only minimally altered levels of BCL-XL or BCL-2. Vincristine treatment in contrast did not induce major changes in expression of these proteins (Fig. 3F). To further substantiate that these observations are relevant in combination with ABT-263, we used a lentiviral CRISPR-Cas9 system to knock-out BCL-2, BCL-XL and MCL-1 with 2 independent sgRNAs each (Fig. 4A) and treated knock-out cells with ABT-263 for 24h. Remarkably, cells lacking MCL-1 exhibited a strongly sensitized drug response consistent with previous reports [11], and phenocopied effects detected in wildtype cells upon combination treatment with ABT-263 and standard chemotherapeutics (Fig. 4B). Hence, the data suggest a model where BCL-XL and MCL-1 are the 2 major proteins mounting the anti-apoptotic response in recurrent RMS cells. To validate this vulnerability, we pharmacologically inhibited both BCL-XL and MCL-1 using the specific inhibitors A-1331852 (BCL-XLi) and A-1210477 (MCL-1i). This drug combination severely inhibited cell growth in a synergistic manner in 3 relapse PPCs, similar to the ABT-263/standard chemotherapy treatment (Fig. 4C). Importantly, while the combination of

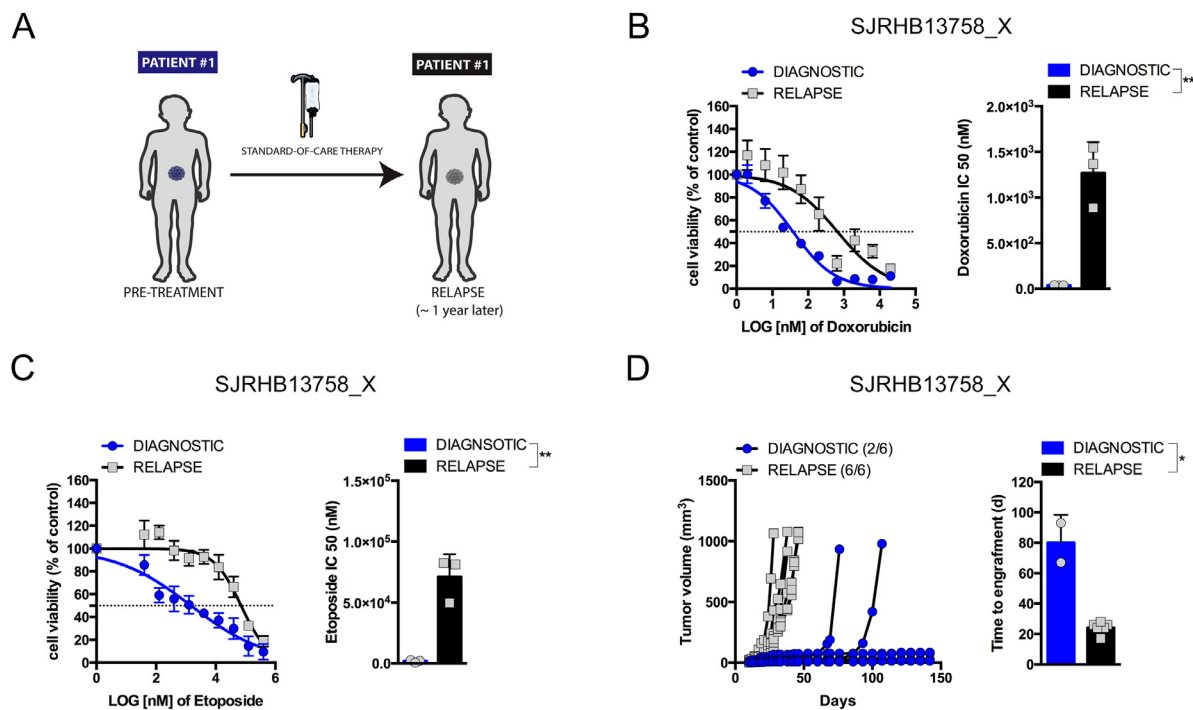


**Fig. 1.** PDX-derived primary cultures from paired diagnostic and relapse rhabdomyosarcoma tumors (A) Representation of a case study of a patient at time of diagnosis and relapse. PPCs were derived from corresponding pre- and post-treatment PDX samples (SJRHB13758\_X1 and SJRHB13758\_X2, respectively). (B and C, left panel) Dose response curves of diagnostic (SJRHB13758\_X1C, blue) and relapse (SJRHB13758\_X2C, gray) cells following 72h treatment with doxorubicin (B) and etoposide (C). (B and C, right panel) Histogram showing the corresponding IC-50 values for each drug. (Mean  $\pm$  sd; N = 3; 2-tailed unpaired *t* test;  $**P \leq 0.01$ ). (D, left panel) Tumor growth of diagnostic (blue) and recurrent (gray) PDX samples after implantation in mice (N = 6). (D, right panel) Histogram indicating the d of engraftment for individual mice (gray dots) when tumors reached  $\sim 100$  mm<sup>3</sup>. (Mean  $\pm$  sd; Mann-Whitney 2-tailed *t* test;  $*P \leq 0.05$ ) (Color version of the figure is available online.)

the 2 drugs was very effective, single drug treatments did not significantly affect cell viability, resulting in very high BLISS synergy scores of nearly 50 in 2 samples (Fig. 4C).

We then investigated which of the pro-apoptotic proteins is engaged by ABT-263/standard chemotherapy. We initially focused on NOXA, because it is a well-known MCL-1 antagonist and has been shown to be involved in sensing different types of stress in RMS cells [12-16]. Thus, we knocked-out NOXA in SJRHB13758\_X2C cells using CRISPR-Cas9 (Fig. 5A) and assessed both caspase activity and cell viability after combination treatment. Interestingly, NOXA depletion significantly attenuated apoptosis after short term combination treatment (3 to 24h) of ABT-263 with both doxorubicin and vincristine compared to control cells (Fig. 5B and 5C and Supplemental Fig. S4A), and rescued cell survival after 72h (vincristine) or 24h (doxorubicin) (Fig. 5D and Supplemental Figure S4B). Consistent with this, NOXA protein levels were transiently and shortly (6 to 9h) upregulated upon exposure to cytotoxic agents (Fig. 5E), correlating with the peak of cell death observed at early time points in combinatorial treatments (Fig. 2D and 2E).

#### ABT-263 enhances response to chemotherapeutics in vivo.

To evaluate the ABT-263/chemotherapy combination in a pre-clinical *in vivo* model of resistant RMS, we treated SJRHB13758\_X2 PDX harboring mice. We administered ABT-263 for 5 consecutive d (d1 to 5) and vincristine for 2 d (d1 and 4) alone and in combination for a total of 3 wk. Although we did not achieve tumor regression in any of the mouse cohorts, the combination significantly delayed tumor growth and prolonged animal

survival when compared to vincristine-only treated mice (Fig. 6A). Hence, these data suggest that ABT-263 combined with first-line therapy can exploit the BCL-XL/MCL-1/NOXA axis to delay tumor growth and represents a valuable strategy for relapsed FN-RMS patients.

Collectively, these findings suggest a model whereby chemotherapeutic treatment induces NOXA while antagonizing MCL-1, whereas ABT-263 targets BCL-XL to promote cell death (Fig. 6B).

Overall, the data presented here demonstrate that the mitochondrial apoptotic pathway represents a relevant vulnerability in combination with standard chemotherapeutics in this molecularly otherwise hard to target tumor.

## Discussion

Using our recently established drug profiling platform for primary cultures, we aimed here to identify novel combinatorial therapy options for high-risk RMS patients who continue to experience insufficient clinical benefit from combinations of standard debulking agents including VAC, VAC plus topoisomerase inhibitors or VAC plus carboplatin [2]. We identified ABT-263 as the top-scoring drug capable of restoring vulnerability to a range of cytotoxic agents (i.e. doxorubicin, etoposide and vincristine) and enhancing response to chemotherapy *in vivo*. ABT-263 resembles the structure of the BH3-only protein BAD, thus is designed to induce apoptosis by neutralizing the pro-survival function of the BCL-2 family members BCL-2, BCL-XL and BCL-W [17]. We found that inhibition of BCL-XL is likely to contribute to the cooperativity of ABT-263 with standard chemotherapy. This has been demonstrated by the increased sensitivity of PPCs toward

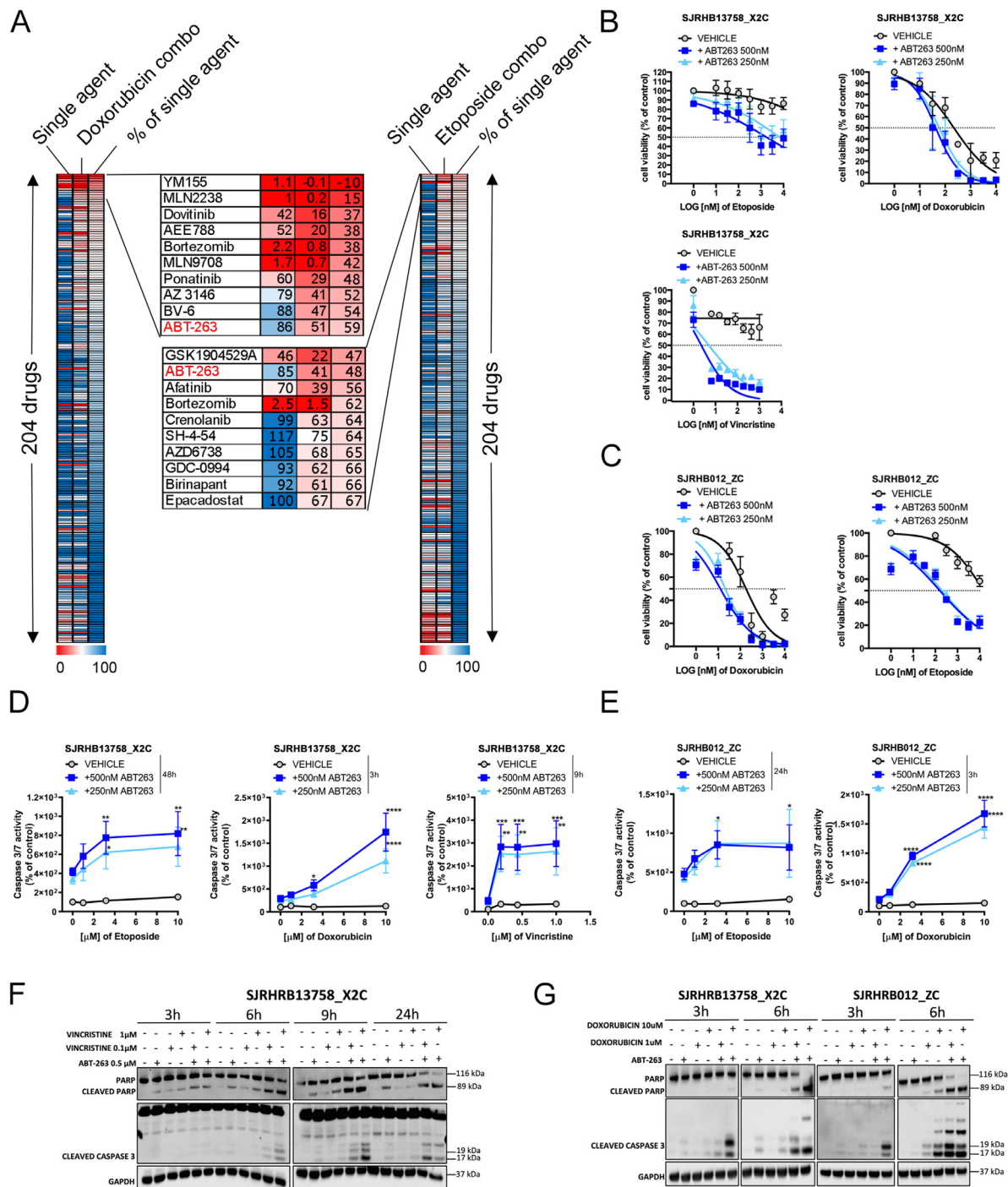


**Fig. 2.** Combination screen identifies ABT-263 as re-sensitizer of recurrent PPCs to first-line treatments  
 (A) Heatmap depicting the results of the drug screen aimed at identifying compounds that modulate the sensitivity to doxorubicin (left panel) and etoposide (right panel) in SJRHB13758\_X2C cells. Top ten hit compounds are depicted in enlarged boxes in the middle. The common candidate (ABT-263) is highlighted in red. Numbers refer to cell viability as measured by WST assay and normalized to the vehicle-treated control.  
 (B) Viability of SJRHB13758\_X2C cells treated with increasing concentrations of etoposide, doxorubicin and vincristine alone (black) or in combination with ABT-263 (500nM and 250nM, dark and light blue lines, respectively) for 72h. (Mean  $\pm$  sd; N = 3-4). (C) Cell viability of SJRHB012\_ZC PPCs co-treated with or without ABT-263 (250nM and 500nM) and increasing concentrations of doxorubicin (left panel, mean  $\pm$  sd; N = 2) or etoposide (right panel, mean  $\pm$  sd; N = 4) for 72h. (D) Caspase 3/7-activity assay performed in SJRHB13758\_X2C cells following treatment with etoposide, doxorubicin and vincristine with or without ABT-263 at indicated time points. (Mean  $\pm$  SD; N = 3; 2-way ANOVA; \* $P \leq 0.05$ ; \*\* $P \leq 0.01$ ; \*\*\* $P \leq 0.001$ ; \*\*\*\* $P \leq 0.0001$ ). (E) Caspase 3/7-activity assay following treatment of SJRHB012\_ZC cells with indicated chemotherapeutics with or without ABT-263. Time points are also shown. (Mean  $\pm$  sd; N = 2-3; 2-way ANOVA; \* $P \leq 0.05$ ; \*\* $P \leq 0.01$ ; \*\*\* $P \leq 0.001$ ; \*\*\*\* $P \leq 0.0001$ ). (F and G) Western blot analysis showing protein levels of PARP, cleaved PARP and cleaved CASPASE 3 after short-term exposure of PPCs to single or combinatorial treatments with indicated compounds. GAPDH was used as loading control (Color version of the figure is available online).

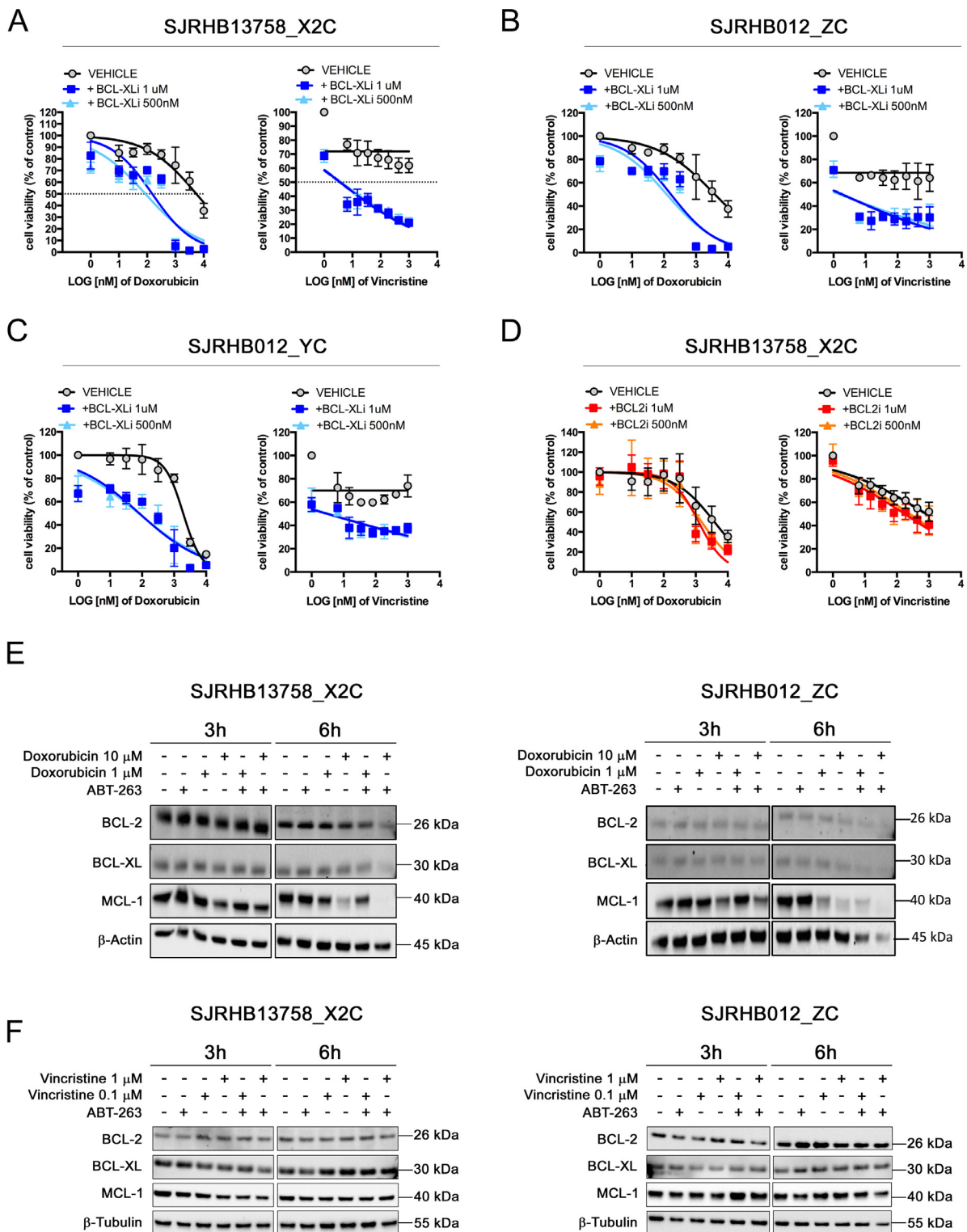


**Fig. 3.** Selective inhibition of BCL-XL mimics the effect of ABT-263 in PPCs. (A-C) Dose response curves of indicated cells co-treated with a selective BCL-XL inhibitor (BCL-XLi, A-1331852) at 500nM (light blue) or 1uM (dark blue) and increasing concentrations of doxorubicin (left panel) or vincristine (right panel) for 24h. (Mean  $\pm$  sd; N = 2-3). (D) Cell viability analysis of SJRHB13758\_X2C cells co-treated with a specific BCL-2 inhibitor (BCL-2i) (ABT-199) at 500nM (orange) or 1uM (red) and doxorubicin (left panel, N = 2) or vincristine (right panel, N = 3) for 24h. (Mean  $\pm$  sd). (E) Western blot analysis showing the expression of indicated proteins after treatment with ABT-263 (500nM) and/or doxorubicin (1 $\mu$ M and 10 $\mu$ M) in SJRHB13758\_X2C (left panel) and SJRHB012\_ZC (right panel) cells at indicated time points.  $\beta$ -ACTIN was used as loading control. (F) Western blot analysis showing the expression of indicated proteins after treatment with ABT-263 (500nM) and/or vincristine (0.1  $\mu$ M and 1 $\mu$ M) in SJRHB13758\_X2C (left panel) and SJRHB012\_ZC (right panel) cells at indicated time points.  $\beta$ -Tubulin was used as loading control (Color version of the figure is available online.).

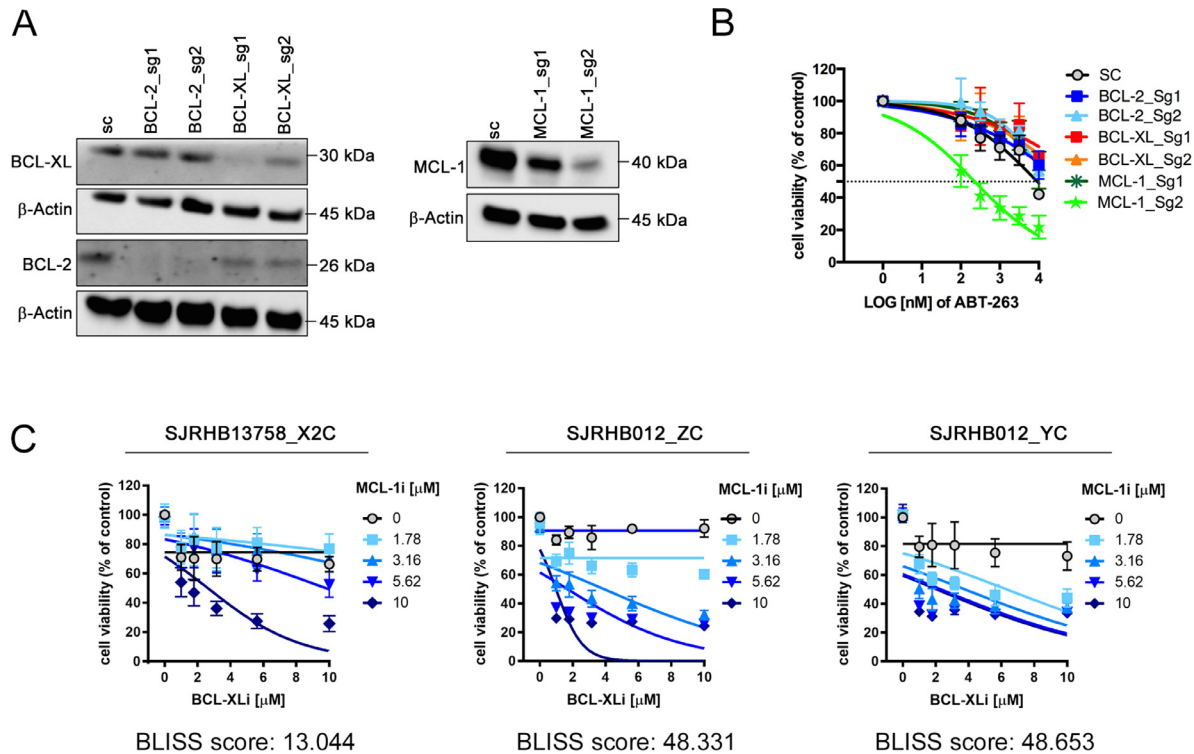


**Fig. 4.** Genetic interference with BCL-XL phenocopies the effect of ABT-263 in PPCs. (A) Western blot detection of indicated proteins using cell extracts of SJRHB13758\_X2C cells transduced with CRISPR vectors carrying a scrambled sgRNA (SC) or sgRNAs targeting BCL-2, BCL-XL (left panel) and MCL-1 (right panel).  $\beta$ -ACTIN was used as loading control. (B) Cell viability assay performed with SJRHB13758\_X2C cells depleted of BCL-2 (light and dark blue lines), BCL-XL (red and orange lines) and MCL-1 (light and dark green lines) and treated with increasing concentrations of ABT-263 for 24h. (Mean  $\pm$  sd; N = 2-3). (C) Cell viability of indicated cells upon treatment with a BCL-XLi (A-1331852) and a MCL-1 (MCL-1i, A-1210477) inhibitor for 72h. (Mean  $\pm$  sd; N = 3) (Color version of the figure is available online.).

doxorubicin and/or vincristine upon pharmacologic interference with BCL-XL and expands the relevance of BCL-XL also to FN-RMS, besides its well-recognized role as modulator of the anti-apoptotic function of PAX3-FOXO1 in FP-RMS [18]. Similar findings have recently been reported in RMS cell lines [19] and are in agreement with other studies that collectively suggest that BCL-XL together with MCL-1 are the more important pro-survival proteins in solid tumors, whereas BCL-2 is more relevant in some leukemia like AML [20]. Indeed, we found BCL-2 to be largely dispensable for the observed phenotype, but detected a functional role for MCL-1 in FN-RMS. We found that the dual inhibition of BCL-XL and MCL-1 represents a “druggable” vulnerability in recurrent PPCs, suggesting that the 2 proteins have redundant functions. This has recently also been described in cell lines of different types of sarcoma including RMS as well as in a range of other solid tumors including melanoma, breast, and lung cancer [21-24]. Clinically, however, such a combination might be problematic due to acute liver toxicity recently detected in mouse models [23].

Our PPCs have been molecularly characterized to resemble primary tumors more closely than established cell lines [9]. Hence, expression of BCL-2 family members is also expected to play an important role in human patient tumors. In support of this, overexpression of *Mcl-1* RNA in 14 primary RMS tumors has been recognized earlier [25] and suggested as novel therapeutic target in sarcomas [26]. Similarly, high level of BCL-XL expression was detected by immunohistochemistry in >60% of RMS tumors (data not shown) and dynamic BH3 profiling predicted chemotherapy sensitivity in 3 RMS cell lines [27], supporting our notion of re-sensitization to first-line therapy.

Our molecular studies further revealed that ABT-263 augments the cytotoxicity of conventional chemotherapeutics via an axis that at least partially relies on NOXA. While NOXA knock-outs did not completely rescue from apoptosis, suggesting that to some extent also other pro-apoptotic players are involved, we did not find any cell death alteration in BIM knock-out cells treated with either ABT-263 alone or with chemotherapy (data not shown), albeit BIM has been proposed as a key determinant of the sensitivity to ABT-263 in a large collection of cancer cell lines [28]. NOXA has already been recognized as a major stress sensor in both FP-RMS and FN-RMS, initiating mitochondrial apoptosis downstream of several types of treatments [12-16,29]. This suggests that NOXA is the main BH3-only stress sensor in most RMS cells.

Interestingly, when performing the combination screens with doxorubicin and etoposide, the compounds BV-6 and birinapant were identified as additional hits, respectively. Both these drugs are second mitochondria-derived activator of caspase (SMAC) mimetics, a type of drug with similarity to the SMAC family of proteins targeting inhibitor of apoptosis proteins (IAPs). Blockade of IAPs therefore releases breaks active in the apoptotic cascade. Hence, SMAC mimetics potentially offer another opportunity for re-sensitization of RMS toward first-line therapies.

From a clinical point of view, BH3-mimetics (ABT-263, its predecessor ABT-737 or the selective BCL-2 inhibitor ABT-199) have previously been shown to potentiate the efficacy of a variety of clinically relevant compounds in a large set of cancer entities [17,28,30-34]. Unfortunately, in contrast to ABT-199, which is well tolerated and clinically approved for the treatment of different types of leukemia, early clinical tests of ABT-

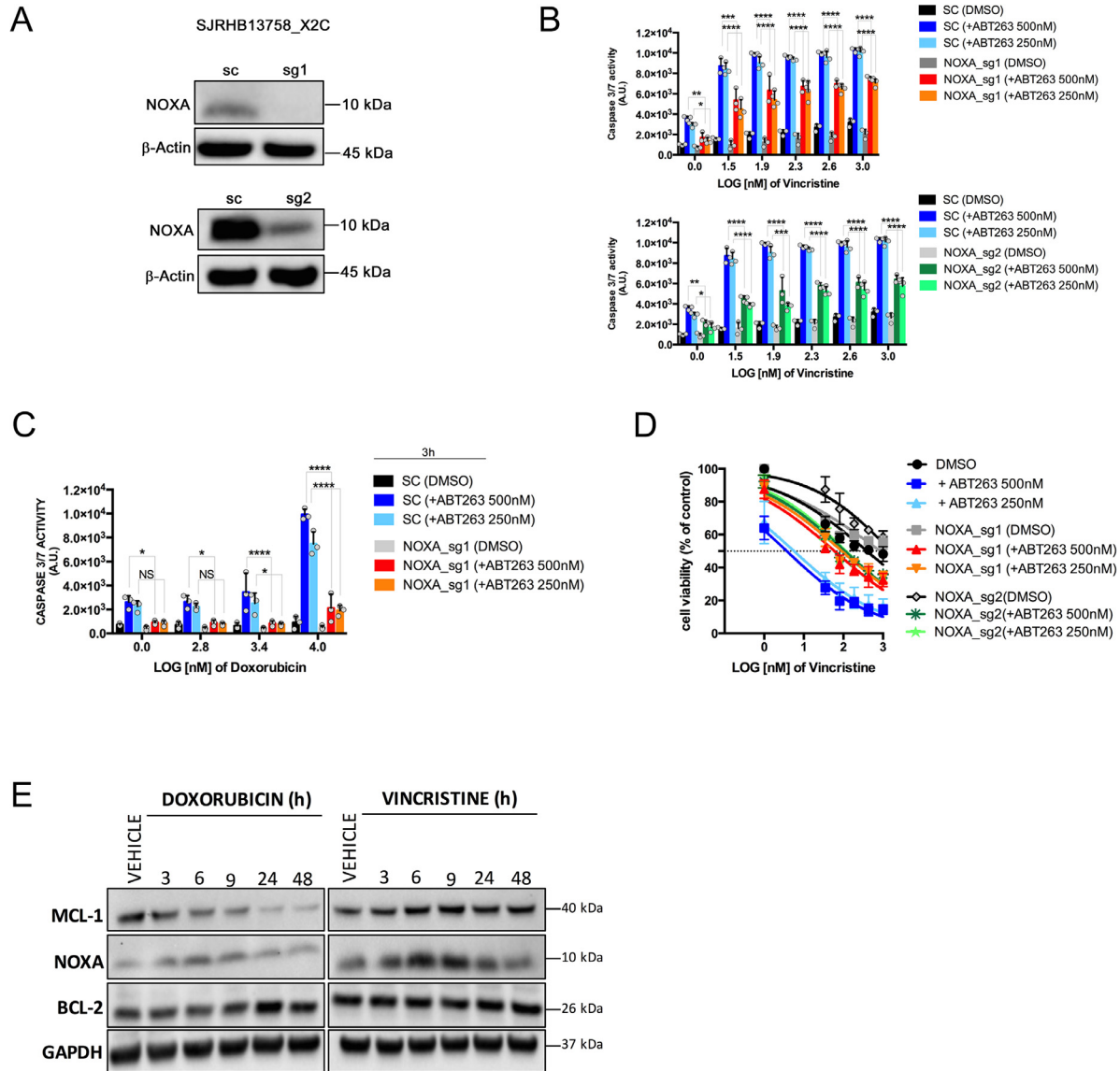


**Fig. 5.** NOXA is a relevant player of the ABT-263-mediated sensitization to chemotherapy. (A) Western blot analysis for validation of NOXA protein depletion upon transduction of SJRHB13758\_X2C cells with CRISPR vectors containing sgRNAs targeting NOXA (sg1 and sg2).  $\beta$ -ACTIN was used as loading control. (B) Caspase 3/7 assay performed with SJRHB13758\_X2C NOXA knock-out cells (sg1, upper panel and sg2, lower panel) upon co-treatment with vincristine and ABT-263 (500nM and 250nM) for 24h. (Mean  $\pm$  sd; N = 3; 2-way ANOVA; \* $P \leq 0.05$ ; \*\* $P \leq 0.01$ ; \*\*\* $P \leq 0.001$ ; \*\*\*\* $P \leq 0.0001$ ; NS, not significant). (C) Caspase 3/7 assay performed on SJRHB13758\_X2C NOXA knock-out cells upon co-treatment with doxorubicin and ABT-263 (500nM and 250nM) for 3 hours. (Mean  $\pm$  sd; N = 3; 2-way ANOVA; \* $P \leq 0.05$ ; \*\* $P \leq 0.01$ ; \*\*\* $P \leq 0.001$ ; \*\*\*\* $P \leq 0.0001$ ; NS, not significant). (D) WST-1-assay performed on SJRHB13758\_X2C NOXA knock-out cells upon treatment with increasing concentrations of vincristine for 72h. (E) Western blot detection of MCL-1, NOXA, and BCL-2 using extracts from SJRHB13758\_X2C cells treated with either doxorubicin (left) or vincristine (right) for 3, 6, 9, 24, and 48 hours (H). GAPDH was used as loading control.

263 have shown that it induces thrombocytopenia via on-target effects in platelets, limiting its clinical use [35]. However, combinatorial approaches as described here open the possibility to use lower doses that might spare platelets to a large extent. Furthermore, recent studies with a PROTAC-version of ABT-263, mediating BCL-XL degradation via recruitment to the von Hippel-Lindau (VHL) E3 ligase, have shown that in such an approach platelets are much less affected by the drug, since these do not express VHL [36].

Taken together, these results strongly suggest that clinical use of BCL-XL directed drugs should be reconsidered in the future for therapy of RMS.

## Material and methods

### PDX transplantation

PDX tumors were transplanted as described previously [9]. For tumor amplification, pieces with a size of ~10 to 30 mm<sup>3</sup> from fresh human tumor biopsies or established PDX tumors were transplanted subcutaneously into the flank of 6 to 10 wk old, sex-matched NOD scid gamma (NSG) mice. Engraftment of tumors was monitored by tumor size measurements 3 times a wk using a caliper. Tumors were isolated when they reached a size of ~1000 mm<sup>3</sup>.

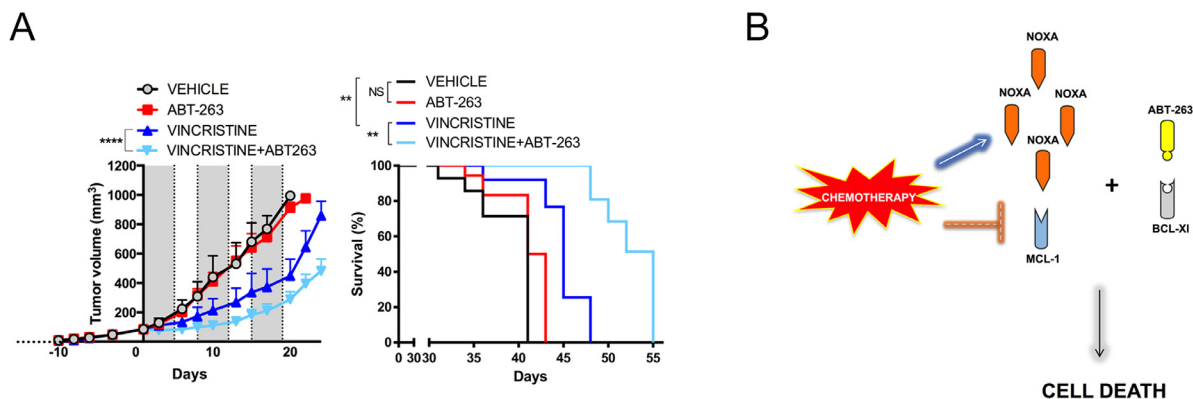


**Fig. 6.** ABT-263 augments the effect of chemotherapy *in vivo*. (A, left panel) Tumor growth curves of SJRHB13758\_X2 PDX following vehicle application (black line) or treatment with ABT-263 only (red line), vincristine only (dark blue) and the combination (light blue). Gray color indicates time of therapy (3 wk). (Mean  $\pm$  sem; N = 6; 2-way ANOVA; \*\*\*\* $P \leq 0.0001$ ). (A, right panel) Survival curve of mice from left panel. (Log rank (Mantel-Cox) test; \* $P \leq 0.05$ ; \*\* $P \leq 0.01$ ; \*\*\* $P \leq 0.001$ ; \*\*\*\* $P \leq 0.0001$ ). (B) Scheme depicting the proposed molecular mechanism underlying the effect of the ABT-263/chemotherapy combination (Color version of the figure is available online.).

For *in vivo* drug treatment, a single cell suspension of dissociated PDX tumors containing 0.7 to  $5 \times 10^6$  cells was injected subcutaneously into the flank of sex matched, 6 to 10 wk old NSG mice.

#### Culture of PDX cells

PDX-derived cells were cultured *in vitro* as described previously [9]. Briefly, FN-RMS PDX cells were cultured on matrigel- or gelatin-coated dishes in NB medium (Thermofisher Scientific, 21103049), supplemented with 2xB-27 (Thermofisher Scientific, 17504044), 100 U/mL penicillin/streptomycin and 2 mM glutamax (Life technologies, 35050-061). Three times per wk, medium was replaced with fresh one. When reaching confluency, cells were detached using Accutase (Sigma-Aldrich, A6964), and splitted in a ratio of 1:2 to 1:3.

For matrigel-coating, matrigel (Corning, 354234) was diluted 1:10 in NB medium and left on the dish for 30 to 60 min at RT. Before cell-plating, excess matrigel solution was removed. For gelatin-coating, a 2% solution of gelatin (Sigma-Aldrich, G9391) in water was left on the dish for 2h at 37°C. The solution was then removed and the plates were dried at RT for 30 to 60 min.

#### Drug profiling

For drug profiling, 3000 to 20000 PPCs were plated per 384 well. The next d, medium was changed, and cells were incubated with a drug library containing 204 different drugs (Selleckchem) in a concentration of 500 nM alone or together with 100 nM vincristine or 1  $\mu$ M etoposide in duplicate wells for 72 h. 12 wells treated with DMSO on each plate served as controls. Cell viability was then determined by WST-1 assay (Roche, 11644807001). A list of compounds employed in this study is provided in Supplemental table 1.

#### Drug response curves

For IC<sub>50</sub> determination 3000 to 20000 PDX cells were plated per 384 well. The next d, medium was changed, and cells were incubated with the drug in a logarithmic concentration range between 0.006 and 10  $\mu$ M using a digital dispenser (HP D300). After 72h cell viability was measured by WST-1 assay.

#### Caspase 3/7-activity assay

Cells were seeded in white 384-well plates with clear bottom (Greiner Bio-One, #781098). Caspase activity was determined at indicated time points by Caspase-Glo 3/7 Assay (Promega, #G8093) according to the manufacturer's instructions. Luminescence was measured using the multidetection microplate reader Synergy HT (Bio-Tek Instruments).

#### In vivo drug treatment

Tumors were established from dissociated PDX and tumor harboring mice were randomized into treatment and control cohorts of 6 animals when the tumor average size reached about 100 mm<sup>3</sup>. ABT-263 (ApexBio, A3007) was dissolved in a mixture of 10% EtOH, 30% PEG-400 (Lipoid) and 60% phosal 50 PG (Sigma Aldrich) and was given orally (100 mg/kg) alone or 1.5 h after standard chemotherapy in combination experiments. Compound solution was prepared fresh before drug administration and any remaining solution was routinely stored at +4°C for no longer than 1 wk. Vincristine (Teva) was injected intravenously (i.v.) (0.5 mg/kg). Tumor size was measured 3 times a wk using a caliper and mouse weight was measured twice a wk. No mice needed to be euthanized due to severe body weight loss (>20% than baseline). All animal experiments were performed under license of the authorities of the Kt. Zürich (206/15).

#### Generation of gene knock-outs by CRISPR-Cas9

Single guide RNAs were designed using the CRISPOR online design tool and cloned by Golden Gate cloning into the plentiCRISPR-EGFP vector (Addgene #75159). Lentiviral particle generation was performed as previously described [37]. Target cells were transduced with sgRNA constructs with an efficiency of 80% to 90%. Cells were then cultured for at least 1 wk before knock-out efficiency was determined by Western Blot and physiological experiments were performed.

SgRNA sequences (without protospacer adjacent motif (PAM)):

SCRAMBLED: GCACTACCAGAGCTAACTCA  
MCL-1 sg1: CTCAAAAGAAACGCGGTAAT  
MCL-1 sg2: TGGAGACCTTCCAGCCGGTT  
BCL-XL sg1: CAGTGGCTCCATTACCAGCGG  
BCL-XL sg2: GGGTTGCCATTGATGGCACT  
BCL-2 sg1: GAGAACAGGGTACGATAACC  
BCL-2 sg2: GTCGCAGAGGGGCTACGAGT



NOXA sg1: ACGCTCAACCGAGCCCCGCG  
NOXA sg2: TCGAGTGTGCTACTCAACTC

### Western blot

Generation of cell lysates using RIPA buffer and protein detection by Western blot was performed as described previously [38]{Bohm, 2016 #30}. Antibodies used in this study included: anti-GAPDH (#2118S; Cell Signaling), anti-PARP (#9542S; Cell Signaling), anti-cleaved CASPASE 3 (#9664P; Cell Signaling), anti-BCL-XL (#2762S; Cell Signaling), anti-MCL-1 (#5453T; Cell Signaling), anti-NOXA (#14766S; Cell Signaling), anti  $\beta$ -ACTIN (#12262S, HRP-conjugated; Cell Signaling) and anti-BCL-2 (#M0887; Dako). All primary antibodies were diluted 1:1000 in milk. For secondary antibodies, HRP-linked anti-mouse IgG (Cell Signaling, #7076S) and HRP-linked anti-rabbit IgG (Cell Signaling, #7074S) were used at 1:5000 dilution in milk.

### Bioinformatic analysis and statistics

Data analysis was performed using GraphPad Prism (version 6). Statistic tests and number of biological replicates (N) per each experiment are outlined in figure legends. BLISS synergy scores were calculated using the Synergyfinder webtool (<https://synergyfinder.fimm.fi>)

### Authors' contributions

*Gabriele Manzella*: Conceptualization; Data curation; Investigation; Methodology; Writing – original draft. *Devmini C. Moonamale*: Data curation; Investigation. *Michaela Römmele*: Data curation; Formal analysis; Investigation; Methodology. *Peter Bode*: Data curation; Investigation. *Marco Wachtel*: Conceptualization; Data curation; Investigation; Methodology; Writing – original draft, review & editing. *Beat W. Schäfer*: Conceptualization; Data curation; Funding acquisition; Project administration; Supervision; Validation; Writing – review & s.

### Supplementary materials

Supplementary material associated with this article can be found, in the online version, at doi:10.1016/j.neo.2021.07.001.

### References

[1] Housman G, Byler S, Heerboth S, Lapinska K, Longacre M, Snyder N, Sarkar S. Drug resistance in cancer: an overview. *Cancers (Basel)* 2014;**6**:1769–92.  
[2] Hawkins DS, Spunt SL, Skapek SX, Committee COGSTS. Children's oncology group's 2013 blueprint for research: soft tissue sarcomas. *Pediatr Blood Cancer* 2013;**60**:1001–8.  
[3] Raney RB Jr, Crist WM, Maurer HM, Foulkes MA. Prognosis of children with soft tissue sarcoma who relapse after achieving a complete response. A report from the Intergroup Rhabdomyosarcoma Study I. *Cancer* 1983;**52**:44–50.  
[4] Crist W, Gehan EA, Ragab AH, Dickman PS, Donaldson SS, Fryer C, Hammond D, Hays DM, Herrmann J, Heyn R, et al. The third intergroup rhabdomyosarcoma study. *J Clin Oncol* 1995;**13**:610–30.  
[5] Gillet JP, Varma S, Gottesman MM. The clinical relevance of cancer cell lines. *J Natl Cancer Inst* 2013;**105**:452–8.  
[6] Ben-David U, Siranosian B, Ha G, Tang H, Oren Y, Hinohara K, Strathdee CA, Dempster J, Lyons NJ, Burns R, et al. Genetic and transcriptional evolution alters cancer cell line drug response. *Nature* 2018;**560**:325–30.  
[7] Drost J, Clevers H. Organoids in cancer research. *Nat Rev Cancer* 2018;**18**:407–18.  
[8] Byrne AT, Alferez DG, Amant F, Annibaldi D, Arribas J, Biankin AV, Bruna A, Budinska E, Caldas C, Chang DK, et al. Interrogating open issues

in cancer precision medicine with patient-derived xenografts. *Nat Rev Cancer* 2017;**17**:254–68.  
[9] Manzella G, Schreck LD, Breunis WB, Molenaar J, Merks H, Barr FG, Sun W, Rommele M, Zhang L, Tchinda J, et al. Phenotypic profiling with a living biobank of primary rhabdomyosarcoma unravels disease heterogeneity and AKT sensitivity. *Nat Commun* 2020;**11**:4629.  
[10] Merino D, Kelly GL, Lessene G, Wei AH, Roberts AW, Strasser A. BH3-mimetic drugs: blazing the trail for new cancer medicines. *Cancer Cell* 2018;**34**:879–891.  
[11] van Delft MF, Wei AH, Mason KD, Vandenberg CJ, Chen L, Czabotar PE, Willis SN, Scott CL, Day CL, Cory S, et al. The BH3 mimetic ABT-737 targets selective Bcl-2 proteins and efficiently induces apoptosis via Bak/Bax if Mcl-1 is neutralized. *Cancer Cell* 2006;**10**:389–99.  
[12] Willis SN, Chen L, Dewson G, Wei A, Naik E, Fletcher JI, Adams JM, Huang DC. Proapoptotic Bak is sequestered by Mcl-1 and Bcl-xL, but not Bcl-2, until displaced by BH3-only proteins. *Genes Dev* 2005;**19**:1294–305.  
[13] Heinicke U, Kupka J, Fichter I, Fulda S. Critical role of mitochondria-mediated apoptosis for JNJ-26481585-induced antitumor activity in rhabdomyosarcoma. *Oncogene* 2016;**35**:3729–41.  
[14] Graab U, Hahn H, Fulda S. Identification of a novel synthetic lethality of combined inhibition of hedgehog and PI3K signaling in rhabdomyosarcoma. *Oncotarget* 2015;**6**:8722–35.  
[15] Meister MT, Boedicker C, Graab U, Hugle M, Hahn H, Klingebiel T, Fulda S. Arsenic trioxide induces Noxa-dependent apoptosis in rhabdomyosarcoma cells and synergizes with antimicrotubule drugs. *Cancer Lett* 2016;**381**:287–295.  
[16] Ramirez-Peinado S, Alcazar-Limones F, Lagares-Tena L, El Mjijad N, Caro-Maldonado A, Tirado OM, Munoz-Pinedo C. 2-deoxyglucose induces Noxa-dependent apoptosis in alveolar rhabdomyosarcoma. *Cancer Res* 2011;**71**:6796–806.  
[17] Tse C, Shoemaker AR, Adickes J, Anderson MG, Chen J, Jin S, Johnson EF, Marsh KC, Mitten MJ, Nimmer P, et al. ABT-263: a potent and orally bioavailable Bcl-2 family inhibitor. *Cancer Res* 2008;**68**:3421–8.  
[18] Margue CM, Bernasconi M, Barr FG, Schafer BW. Transcriptional modulation of the anti-apoptotic protein BCL-XL by the paired box transcription factors PAX3 and PAX3/FKHR. *Oncogene* 2000;**19**:2921–9.  
[19] Faqar-Uz-Zaman SF, Heinicke U, Meister MT, Vogler M, Fulda S. BCL-xL-selective BH3 mimetic sensitizes rhabdomyosarcoma cells to chemotherapeutics by activation of the mitochondrial pathway of apoptosis. *Cancer Lett* 2018;**412**:131–42.  
[20] Soderquist RS, Crawford L, Liu E, Lu M, Agarwal A, Anderson GR, Lin KH, Winter PS, Cakir M, Wood KC. Systematic mapping of BCL-2 gene dependencies in cancer reveals molecular determinants of BH3 mimetic sensitivity. *Nat Commun* 2018;**9**:3513.  
[21] Kehr S, Haydn T, Bierbrauer A, Irmer B, Vogler M, Fulda S. *Targeting BCL-2 proteins in pediatric cancer: Dual inhibition of BCL-XL and MCL-1 leads to rapid induction of intrinsic apoptosis.* *Cancer Lett*; 2020.  
[22] Lee EF, Harris TJ, Tran S, Evangelista M, Arulananda S, John T, Ramnac C, Hobbs C, Zhu H, Gunasingh G, et al. BCL-XL and MCL-1 are the key BCL-2 family proteins in melanoma cell survival. *Cell Death Dis* 2019;**10**:342.  
[23] Weeden CE, Ah-Cann C, Holik AZ, Pasquet J, Garnier JM, Merino D, Lessene G, Asselin-Labat ML. Dual inhibition of BCL-XL and MCL-1 is required to induce tumour regression in lung squamous cell carcinomas sensitive to FGFR inhibition. *Oncogene* 2018;**37**:4475–88.  
[24] Xiao Y, Nimmer P, Sheppard GS, Bruncko M, Hessler P, Lu X, Roberts-Rapp L, Pappano WN, Elmore SW, Souers AJ, et al. MCL-1 Is a key determinant of breast cancer cell survival: validation of MCL-1 dependency utilizing a highly selective small molecule inhibitor. *Mol Cancer Ther* 2015;**14**:1837–47.  
[25] Pazzaglia L, Chiechi A, Conti A, Gamberi G, Magagnoli G, Novello C, Morandi L, Picci P, Mercuri M, Benassi MS. Genetic and molecular alterations in rhabdomyosarcoma: mRNA overexpression of MCL1 and MAP2K4 genes. *Histol Histopathol* 2009;**24**:61–7.  
[26] Thallinger C, Wolschek MF, Maierhofer H, Skvara H, Pehamberger H, Monia BP, Jansen B, Wacheck V, Selzer E. Mcl-1 is a novel therapeutic target for

- human sarcoma: synergistic inhibition of human sarcoma xenotransplants by a combination of mcl-1 antisense oligonucleotides with low-dose cyclophosphamide. *Clin Cancer Res* 2004;**10**:4185–91.
- [27] Alcon C, Manzano-Munoz A, Prada E, Mora J, Soriano A, Guillen G, Gallego S, Roma J, Samitier J, Villanueva A, et al. Sequential combinations of chemotherapeutic agents with BH3 mimetics to treat rhabdomyosarcoma and avoid resistance. *Cell Death Dis* 2020;**11**:634.
- [28] 3rd Faber AC, Farago AF, Costa C, Dastur A, Gomez-Caraballo M, Robbins R, Wagner BL, Rideout WM, Jakubik CT, Ham J, et al. Assessment of ABT-263 activity across a cancer cell line collection leads to a potent combination therapy for small-cell lung cancer. *Proc Natl Acad Sci U S A* 2015;**112**:E1288–96.
- [29] Ommer J, Selfe JL, Wachtel M, O'Brien EM, Laubscher D, Roemmele M, Kasper S, Delattre O, Surdez D, Petts G, et al. Aurora A kinase inhibition destabilizes PAX3-FOXO1 and MYCN and synergizes with navitoclax to induce rhabdomyosarcoma cell death. *Cancer Res* 2020;**80**:832–42.
- [30] Anderson GR, Wardell SE, Cakir M, Crawford L, Leeds JC, Nussbaum DP, Shankar PS, Soderquist RS, Stein EM, Tingley JP, et al. PIK3CA mutations enable targeting of a breast tumor dependency through mTOR-mediated MCL-1 translation. *Sci Transl Med* 2016;**8** 369ra175.
- [31] Chen J, Jin S, Abraham V, Huang X, Liu B, Mitten MJ, Nimmer P, Lin X, Smith M, Shen Y, et al. The Bcl-2/Bcl-X(L)/Bcl-w inhibitor, navitoclax, enhances the activity of chemotherapeutic agents in vitro and in vivo. *Mol Cancer Ther* 2011;**10**:2340–9.
- [32] Nakajima W, Sharma K, Hicks MA, Le N, Brown R, Krystal GW, Harada H. Combination with vorinostat overcomes ABT-263 (navitoclax) resistance of small cell lung cancer. *Cancer Biol Ther* 2016;**17**:27–35.
- [33] Preuss E, Hugle M, Reimann R, Schlecht M, Fulda S. Pan-mammalian target of rapamycin (mTOR) inhibitor AZD8055 primes rhabdomyosarcoma cells for ABT-737-induced apoptosis by down-regulating Mcl-1 protein. *J Biol Chem* 2013;**288**:35287–96.
- [34] Roberts AW, Davids MS, Pagel JM, Kahl BS, Puvvada SD, Gerecitano JF, Kipps TJ, Anderson MA, Brown JR, Gressick L, et al. Targeting BCL2 with venetoclax in relapsed chronic lymphocytic leukemia. *N Engl J Med* 2016;**374**:311–22.
- [35] Roberts AW, Seymour JF, Brown JR, Wierda WG, Kipps TJ, Khaw SL, Carney DA, He SZ, Huang DC, Xiong H, et al. Substantial susceptibility of chronic lymphocytic leukemia to BCL2 inhibition: results of a phase I study of navitoclax in patients with relapsed or refractory disease. *J Clin Oncol* 2012;**30**:488–96.
- [36] Khan S, Zhang X, Lv D, Zhang Q, He Y, Zhang P, Liu X, Thummuri D, Yuan Y, Wiegand JS, et al. A selective BCL-XL PROTAC degrader achieves safe and potent antitumor activity. *Nat Med* 2019;**25**:1938–47.
- [37] Bohm M, Wachtel M, Marques JG, Streiff N, Laubscher D, Nanni P, Mamchaoui K, Santoro R, Schafer BW. Helicase CHD4 is an epigenetic coregulator of PAX3-FOXO1 in alveolar rhabdomyosarcoma. *J Clin Invest* 2016;**126**:4237–49.
- [38] Oesch S, Walter D, Wachtel M, Pretre K, Salazar M, Guzman M, Velasco G, Schafer BW. Cannabinoid receptor 1 is a potential drug target for treatment of translocation-positive rhabdomyosarcoma. *Mol Cancer Ther* 2009;**8**:1838–45.